energies

MDPI

Article

Efficient Charging Prioritisation and Optimisation of Solar PV-Powered Portable Electronic Devices

Tawanda Kunatsa *, Herman C. Myburgh and Allan De Freitas

Department of Electrical, Electronic and Computer Engineering, University of Pretoria, Pretoria 0002, South Africa; herman.myburgh@up.ac.za (H.C.M.); allan.defreitas@up.ac.za (A.D.F.)
* Correspondence: tawanda.kunatsa@tuks.co.za; Tel.: +27-84-5622181

Abstract: Efficiently managing and prioritising the charging of portable electronic devices powered by solar photovoltaic sources in off-grid and resource-limited environments is a huge problem. Ensuring that critical devices maintain operational uptime, especially when energy resources are scarce and in instances where multiple devices compete for charging from the limited solar power available is crucial. This paper introduces an optimisation framework designed to prioritise the charging of portable electronic devices powered by solar photovoltaic sources. The approach aims to maximise operational uptime for critical loads before addressing less essential ones. By strategically allocating charging priorities based on comprehensive evaluations of battery capacities, usage patterns, and operational requirements, the optimisation process seeks to enhance overall efficiency and readiness of portable electronic devices in dynamic, austere and resource-constrained settings. The charging prioritisation problem was solved using MATLAB's (version number 9.13.0.2193358 (R2022b)) OPTI toolbox in conjuction with the SCIP solver. A case study, involving three portable electronic devices—a cellphone, GPS and radio, demonstrated the model's effectiveness in maximising satisfaction by aggregating device priorities over time. The model prioritised charging of the GPS due to its critical operational role, followed by the radio for its essential communication function, while the cellphone, with lower usage demands, was assigned the lowest priority. The model developed in this study is versatile and applicable to diverse demand profiles and any number of portable electronic devices. Furthermore, it can be customised to operate effectively in various geographic locations, irrespective of solar radiation levels.

Keywords: optimisation; modelling; charging prioritisation; solar photovoltaic; portable electronic devices

Citation: Kunatsa, T.; Myburgh, H.C.; De Freitas, A. Efficient Charging Prioritisation and Optimisation of Solar PV-Powered Portable Electronic Devices. *Energies* **2024**, *17*, 6039. https://doi.org/10.3390/en17236039

Academic Editor: Hamed Aly

Received: 15 October 2024
Revised: 15 November 2024
Accepted: 26 November 2024
Published: 1 December 2024

1. Introduction

Many sectors of the economy–including healthcare, information technology, manufacturing, and various others are heavily dependent on consistent power and energy supplies [1,2]. Disruptions to these resources can present substantial challenges during operations, affecting everything from daily activities to critical functions. In many regions, manufacturing, healthcare and the military are among the biggest energy consumers, as such managing energy procurement and transportation is a significant financial and logistical challenge [3,4]. As a result, there is a growing shift towards renewable energy technologies (RETs) and other energy-efficient alternatives to mitigate these challenges. One of the RETs that has gained widespread adoption is solar PV technology.

The source of energy for solar PV technology is the sun. It is essential as a clean, sustainable energy source, offering vast potential to address some of the world's most pressing challenges, including climate change and energy accessibility [5]. The energy from the sun (solar energy), harnessed through technologies like photovoltaics and concentrated solar power, provides an alternative to fossil fuels by offering an inexhaustible supply of power that does not produce greenhouse gas emissions during operation [6]. The decentralised nature of solar energy allows for energy access in remote, off-grid and austere locations,

which can have profound effects on economic development and quality of life, particularly in low-income regions [7]. Modern innovations, such as perovskite solar cells, have also made solar energy more affordable, expanding its viability as a primary energy source [8]. The sun's energy is indispensable in global efforts to achieve a low-carbon future, improve energy equity and create a sustainable ecosystem for future generations [9].

Solar PV systems are particularly valued for their versatility and ease of deployment, which make them suitable for various environments [10,11]. Unlike many other RETs, solar PV systems are of low-maintenance and have a relatively long operational life, which is essential for reliability in diverse settings [12]. Additionally, the lightweight and portable nature of solar PV panels allows them to be easily transported and set up in different locations thereby enhancing their usability [13]. Given that solar energy is abundant and available in most regions, solar PV systems provide a sustainable power source that reduces reliance on traditional fuel supply, thus addressing logistical and dependency issues effectively.

A study by Teichert et al., introduced a method to minimise the total cost of ownership for electric vehicle fleets [14]. This method involves selecting the optimal battery size, number of charging stations, and charging power based on factors such as schedule, vehicle characteristics, and environmental conditions. However, this study did not address the optimisation and prioritisation of charging for portable electronic devices (PEDs). Existing research on charging optimisation predominantly focuses on electric vehicles and unmanned aerial vehicles, leaving a notable research gap in the modelling, optimisation, and prioritisation of PEDs, particularly those that utilise solar power [15–21].

Another study by Kovačević et al., focused on optimising a wearable power system (WPS) designed to provide portable power for electronic equipment [22]. The WPS components, which include an internal combustion engine, a permanent magnet three-phase electrical motor/generator, an inverter, lithium batteries, DC-DC converters, and a controller, were optimised to improve efficiency and effectiveness. Despite these advancements, the study did not explore the optimisation or prioritisation of charging for individual PEDs. This leaves a gap in understanding how to best manage the power needs of different PEDs in real-world scenarios.

In our previous research, we developed a method for modelling and optimising power flow management for solar-powered PEDs [23]. This approach used MATLAB and the OPTI toolbox with SCIP as the solver to ensure that solar-powered PEDs received a continuous and sufficient power supply. Despite these efforts, the case study results highlighted challenges such as topographical obstacles (mountains and trees) and the intermittent nature of solar resources, which impacted the effectiveness of power flow management in remote environments. To address these challenges, recommendations included implementing strategies for charging control and load switching, which are the focus of this current study.

Giving priority to the charging of critical PEDs is of utmost importance, particularly in scenarios where power resources are scarce [24]. It is essential to ensure that key devices, such as communication equipment, navigation systems, and medical devices, are charged first to maintain their functionality. These devices are often indispensable for ensuring the safety and effectiveness of operations, especially in challenging and high-stress environments. Potential operational disruptions are avoided by prioritising their charging of the PEDs and the overall accomplishment of the tasks at hand is enhanced [25].

Previous research often fails to consider a range of factors in developing charging prioritisation strategies, focusing narrowly on single aspects while neglecting other potentially important variables [26]. Such limited perspectives diminish the effectiveness and adaptability of charging prioritisation schemes, making them less suitable for real-world applications [27]. Furthermore, existing studies on energy management for PEDs have not adequately addressed the integration of energy management, charging prioritisation and optimisation in dynamic and practical scenarios [28]. Many studies rely heavily on theoretical models and do not offer innovative, practical strategies tailored to the specific

needs of users [29]. Unlike previous research which primarily concentrated on dynamic energy management for unmanned aerial vehicles [30,31], this study provides valuable insights into the challenges faced by users of PEDs, enhancing readiness and mission effectiveness in diverse operational contexts. While existing literature has explored energy management for various applications, few studies have specifically focused on the unique needs and constraints of PEDs in remote or austere settings [23,32,33].

The following are some of the innovations which this current study contributes to addressing the abovementioned research gaps:

- Introduces a dynamic optimisation framework for prioritising the charging of solar-powered PEDs in resource-constrained environments.
- Emphasises device criticality by identifying essential PEDs and prioritising their charging based on their importance in specific operations.
- Incorporates real-time adaptation to adjust charging priorities according to changing battery levels, usage patterns, and energy availability.
- Utilises an optimisation model with a weighted factor approach to allocate energy efficiently, enhancing uptime and functionality of critical PEDs.
- Provides tailored energy management, essential in austere, off-grid environments, where power efficiency is crucial.

The research problem is first clearly defined, identifying the core issues that the study aims to address. Following this, modelling and optimisation techniques are explored, including the creation of an objective function and constraints to handle the complexities involved. A detailed case study is then presented, demonstrating the application of the proposed modelling and optimisation strategy in a real-world context. The findings from the case study are analysed, with a discussion on their implications and significance in relation to the original problem. Finally, a conclusion is given, offering a comprehensive summary of key insights, contributions, and potential directions for future research.

2. Problem Formulation

Optimising the performance and charging prioritisation of portable electronic devices powered by solar PV presents a multifaceted challenge that requires careful problem formulation. At its core, this issue encompasses the need to maximise the operational efficiency of critical devices while harnessing renewable energy sources in often resource-constrained and unpredictable environments [34]. The optimisation aspect involves balancing the energy requirements of various PEDs, such as radios, GPS units and night-vision goggles among others with the intermittent nature of solar power generation. Additionally, considerations must be made for the varying energy demands based on operational objectives, environmental conditions, and specific requirements.

The methodology for modelling and optimising discussed in this study is not restricted to particular PEDs and is not limited to any number of devices. Each PED possesses its own unique electronic requirements and is equipped with a battery of a specific capacity. The solar panel is seamlessly integrated into a compact design, with supplementary foldable solar blankets offering flexibility by functioning either as independent collectors or enhancing the panel's capacity to capture solar irradiance, exemplifying a mobile or small solar PV solution. The primary battery can either be housed within the solar backpack itself or exist as a separate component, allowing for its integration into the backpack structure as needed [23].

Charging prioritisation further complicates this problem by necessitating the development of algorithms and decision-making frameworks such as the one presented in Figure 1 to allocate limited solar-generated power among competing PEDs effectively. Factors such as device criticality, individual PED's demand/consumption profile, time sensitivity of device usage, individual PED's battery level and available sunlight are taken into account to ensure that essential PEDs receive adequate power while minimising downtime and maximising task execution and operational effectiveness. Thus, the problem formulation for optimising and prioritising the charging of solar PV-powered PEDs entails a compre-

hensive approach that addresses technical, logistical, and operational considerations to enhance effectiveness.

In Figure 1, the main battery bank (MBB) receives power from the solar PV system, and the PED batteries receive power directly from the solar PV system as well as the main battery. The PED electronics power demands are supplied by the respective PED batteries.

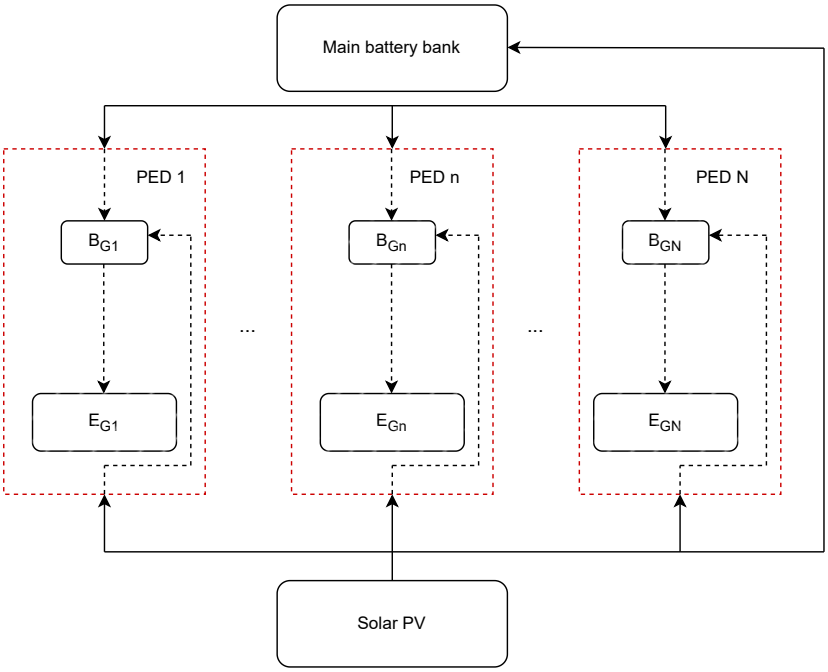

Figure 1. Optimal power flow management framework [23].

3. Modelling and Optimisation

This section presents the modelling and optimisation for PEDs' charging prioritisation. Specific requirements such as charging efficiency, dynamic priority adjustments and other constraints related to charging capabilities and device specifications are also included.

3.1. PV Modelling

The PV generator output can be represented as:

$$P_{pv} = \eta_{pv} A_c I_{pv}, \tag{1}$$

where P_{pv} is the solar PV power output, A_c is the solar PV generator area, η_{pv} is the solar PV generator efficiency which is given by:

$$\eta_{solar} = \eta_{ref}\left[1 - 0.9\mathcal{B}\left(\frac{I_{RR}}{I_{RR,NT}}\right)(T_{c,NT} - T_{A,NT}) - \mathcal{B}(T_A - T_R)\right], \tag{2}$$

where NT represents the nominal cell operating temperature, η_{ref} is the efficiency of the PVs at reference cell temperature, I_{RR} is the solar irradiation incident, $T_{A,NT}$ is the ambient temperature given a nominal cell operating temperature of NT, T_R is the reference cell temperature, and $T_{c,NT}$ is the cell temperature given a nominal cell operating temperature of NT [35].

I_{pv} is the hourly solar irradiation incident on the PV array which can be presented as:

$$I_{pv} = (I_B + I_D)R_B + I_D, \tag{3}$$

where I_B and I_D are the hourly global and diffuse solar irradiation respectively. R_B is the geometrical factor depicting the proportion of beam irradiance incident on a tilted plane to that incident on a horizontal plane [35].

3.2. Battery Modelling

The battery system model comprises the MBB, and the respective batteries for each of the PEDs. The main battery gets power from solar PV and the separate PED batteries get power from the MBB and also directly from the solar PV generator as represented in Figure 1. The energy level of any of the batteries can be presented as follows:

$$E_L(n,t) = E_L(n,0) + \eta_c \sum_{n=1}^{N} P_{F_c} \Delta t(n,t) - \eta_d \sum_{n=1}^{M} P_{F_d} \Delta t(n,t), \tag{4}$$

where E_L is the energy level of the battery, N is the number of PED, η_c and η_d are the battery charging and discharging efficiencies respectively, P_{F_c} and P_{F_d} are the charging and discharging power flows respectively, Δt is the duration of one time slot in hours, n and t are the PED and time interval indices respectively.

The term "state of charge" (SoC) refers to the battery's present charge as a percentage of its total capacity and it describes how fully charged an electrical battery is in relation to its maximum capacity. An SoC of 100% means that the battery is charged to full capacity. SoC changes as the battery charges and discharges. In this study, battery self-discharge is assumed to be negligible. The state of charge of the battery at any particular time ($SoC(n,t)$) is related to the battery energy level at any particular time $E_L(n,t)$ by the following equation:

$$SoC(n,t) = \frac{E_L(n,t)}{Battery\ capacity} \times 100\ \%. \tag{5}$$

Each battery has a minimum allowable capacity SoC^{min} and a maximum allowable capacity SoC^{max} so as to prevent depletion and overcharging of the battery energy storage system (BESS) [36]. This can be presented as follows:

$$SoC^{min} \leq SoC(n,t) \leq SoC^{max}, \tag{6}$$

where $SoC^{max} = DOD \times Battery\ capacity$ and $SoC^{min} = (1 - DOD) \times Battery\ capacity$. DOD is the depth of discharge of the battery and it explains the extent to which a battery is discharged.

3.3. Objective Function

The objective is to maximise the overall satisfaction/utility, which can be represented as the sum of the priorities of all devices over the time horizon. The objective function can be presented as shown below:

$$J = \sum_{i=1}^{M} \sum_{t=1}^{N} \alpha_{i,t}, \tag{7}$$

where $\alpha_{i,t} \in (0,1)$ is the priority of device i at time interval t.

3.4. Constraints

The energy balance equation for each device:

$$B_{i,t} = B_{i,t-1} + (P_{i,t} \times \Delta t) - (R_{i,t} \times C_i \times \Delta t), \tag{8}$$

where $B_{i,t}$ is the battery level of device i at time interval t, $P_{i,t}$ is the power consumed by device i at time interval t, $R_{i,t}$ is the charging rate of device i at time interval t, and C_i is the charging efficiency of device i.

Charging rate constraint:

$$0 \leq R_{i,t} \leq R_{i,max}. \tag{9}$$

Priority adjustment based on battery level and device usage:

$$\alpha_{i,t} = w_i \cdot \left(\frac{B_{i,t}}{B_{max}} + \frac{U_{i,t}}{U_{max}} \right). \tag{10}$$

where w_i is the weighting factor for device i, $U_{i,t}$ is the utilisation of device i at time interval t, and U_{max} is the maximum utilisation among all devices. Equation (10) represents a pivotal element in optimising the charging prioritisation of PEDs powered by solar PV systems. The equation introduces a weighted factor approach to adjust the priority of a specific device at prescribed time intervals based on battery level and utilisation. Combining the normalised battery level and utilisation ensures that the device's priority reflects its energy needs and operational significance. This aligns with the broader objective function, which aims to maximise overall utility by efficiently distributing solar-generated power to critical devices, thereby enhancing operational uptime. The innovation lies in dynamically prioritising charging based on real-time device demands, directly contributing to the main goal of optimising and prioritising the charging of PEDs in resource-constrained environments. This ensures that critical devices receive power first, maintaining their functionality in situations where energy resources are limited. The weighting factor w_i for device i is arrived at as shown in Equations (11) and (12).

$$pr_i = \frac{SPP_i}{BC_i}, \tag{11}$$

where pr_i is the power ratio of the i^{th} device , SPP_i is the sum (Wh) for the i^{th} device and BC_i is the battery capacity(Wh) for the i^{th} device. This ratio is then normalised to get the weighting factor for each PED as follows:

$$norm_i = w_i = \frac{pr_i}{\sum pr} = \frac{\frac{SPP_i}{BC_i}}{\sum\left(\frac{SPP}{BC}\right)}, \tag{12}$$

where $norm_i$ is the normalised ratio which give the values for w_i in Equation (10), $\frac{SPP_i}{BC_i}$ is the power demand relative to the available battery capacity. $\sum pr$ represents the sum of all the $\frac{SPP}{BC}$ values across all devices. This sum normalises the ratio of each individual device, resulting in a normalised value for each device's contribution.

Charging efficiency constraint:

$$R_{i,t} \leq \frac{P_{i,t}}{C_i}. \tag{13}$$

Time horizon constraints:

$$1 \leq t \leq N, \tag{14}$$

$$1 \leq i \leq M, \tag{15}$$

$$0 \leq B_{i,0} \leq B_{max}, \tag{16}$$

$$0 \leq R_{i,t} \leq R_{i,max}, \tag{17}$$

$$0 \leq P_{i,t} \leq P_{i,max}, \tag{18}$$

$$0 \leq P_{i,t} \leq D_{i,t}. \tag{19}$$

where Δt is the time interval, B_{max} is the maximum battery capacity of the device, $R_{i,max}$ is the maximum charging rate of device i and $P_{i,max}$ is the maximum power consumption of device i.

3.5. Optimisation Algorithm

Various optimisation algorithms are available for addressing the PEDs' charging prioritisation problem, in this study, MATLAB is utilised in conjunction with the OPTI Toolbox alongside the SCIP solver. SCIP, recognised for its robustness in tackling mixed-integer nonlinear optimisation problems, seamlessly integrates with MATLAB's OPTI Toolbox, offering a diverse array of optimisation algorithms and techniques [37]. What sets SCIP apart is its capacity to attain a "globally optimal solution", surpassing conventional methods that may only identify local optima. As highlighted by Berthold et al. [38], SCIP excels in thoroughly exploring the solution space, enabling the discovery of globally optimal solutions even in complex optimisation scenarios. The algorithm addresses problems in the following format:

$$min\ f(X),$$

subject to:

$$\begin{cases} AX \leq b \quad \text{(linear inequality constraint)}, \\ AeqX = beq \quad \text{(linear equality constraint)}, \\ C(X) \leq 0 \quad \text{(nonlinear inequality constraint)}, \\ Ceq = 0 \quad \text{(nonlinear equality constraint)}, \\ Lb \leq X \leq Ub \quad \text{(lower and upper bounds)}. \end{cases}$$

4. Case Study

The solar radiation information utilised in this research was acquired from Stellenbosch University's weather station through the Southern African Universities Radiometric Network (SAURAN) [39]. This station employs instruments such as pyranometers or radiometers to gauge solar irradiance, quantifying the amount of solar radiation received per unit area over a specific duration. Figure 2 illustrates a plot of the entire solar irradiance dataset for 18 March 2018, considered by the authors as a typical day. The data from the year 2018 was used in this study as a representative example to illustrate irradiance on a typical day, demonstrating the model's adaptability and optimisation capabilities. The model and optimisation approach herein this study is versatile and is designed to work effectively with data from any year, whether recent or historical. Thus, this example serves to demonstrate the model's functionality rather than imply any restriction to specific data. Employing the average radiometric data for a typical day in modelling facilitates a more precise depiction of overall conditions and trends. Averaging the data across a day, helps to mitigate short-term fluctuations or irregularities that might occur within shorter time intervals. This method enables a more dependable analysis and forecast of long-term patterns and behaviours. Furthermore, utilising data from an average day aids in mitigating the influence of potential measurement errors or discrepancies inherent in individual data points.

It is essential to understand the intricate interplay between battery capacities, utilisation requirements, and the overarching objective of maximising operational efficiency. The respective battery specifications for the PEDs used in this case study are presented in Table 1.

Table 1. Battery specifications [23].

PED	Battery Capacity (mAh)	Battery Voltage (V)
Main battery	10,000	5
Cellphone	2600	5
GPS	5000	3.7
Radio	1600	5

Beginning with battery capacities, the hierarchy among the devices is established based on their respective energy storage capabilities. The GPS, being the device with the highest battery capacity, signifies its capacity to retain a substantial amount of energy. This aspect is crucial, particularly in situations where continuous and uninterrupted operation is paramount for operational success. Following the GPS, the Cellphone assumes the second position in terms of battery capacity, indicating its capacity to hold a moderate amount of charge. Finally, the Radio, with the lowest battery capacity, suggests a comparatively limited capacity for energy storage, necessitating efficient management of its power resources.

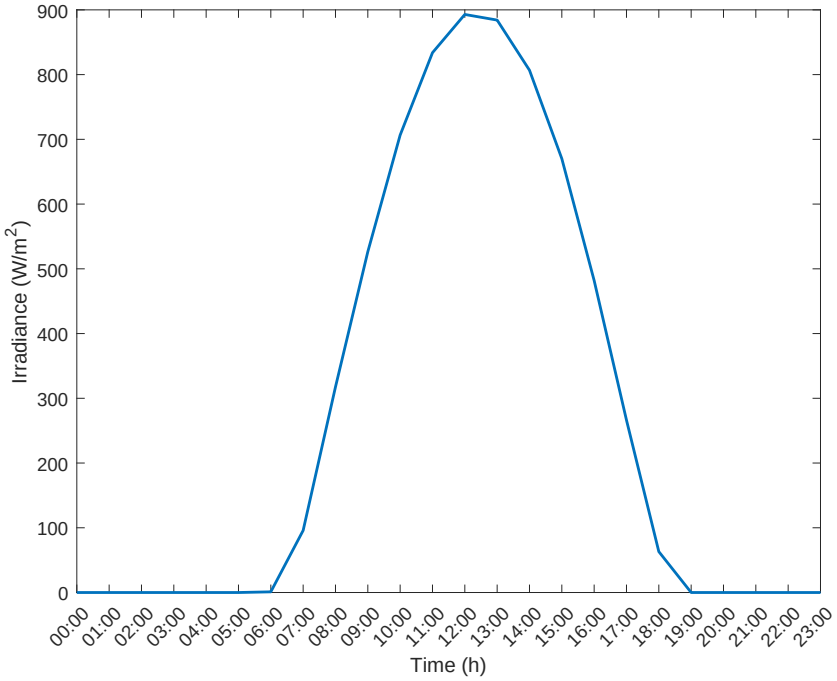

Figure 2. Case solar irradiance [39], 18 March 2018, Latitude: −33.92810059 and Longitude: 18.86540031.

Moving on to utilisation or consumption patterns, this metric provides insights into the intensity of power demands imposed by each device during operation. The respective PEDs consumption profiles used in this case study are presented in Figure 3. The GPS emerges as the most power-intensive device, demanding a significant amount of energy to sustain its functionalities effectively. This heightened utilisation underscores the critical role of the GPS in facilitating navigation, positioning, and other related critical tasks. Following the GPS, the Radio exhibits a notable level of utilisation, albeit lower than that of the GPS. Nevertheless, its requirement for consistent power supply underscores its significance in facilitating communication, coordination, and possibly reconnaissance efforts. Conversely, the Cellphone registers the lowest utilisation among the three devices, indicating relatively lower power demands compared to the GPS and Radio.

Weighting factors and normalisation are integral aspects in the modelling and optimisation of complex problems, such as maximising the sum of battery levels and utilisation to prioritise charging of solar-powered PEDs [40]. These techniques play crucial roles in balancing objectives, as weighting factors enable the assigning of relative importance to different components of the objective function [41]. For instance, ensuring that one specific device is fully charged might hold higher priority compared to other less critical devices, and appropriate weights ensure the optimisation algorithm focuses on satisfying the most critical and crucial objectives while still considering secondary goals. Moreover, normalisation ensures consistency across variables or parameters with different units or scales, standardising them to a common scale [42]. In the charging prioritisation scenario, where battery levels and device utilisation vary in measurement units or ranges, normalisation ensures each component of the objective function contributes meaningfully to the optimi-

sation process, preventing any single variable from dominating due to scale differences. By employing weighting factors and normalisation, biases in the optimisation algorithm are mitigated, ensuring a fair and balanced approach to achieving an optimal solution. This technique also offers flexibility and adaptability, allowing for adjustments in priorities or constraints as mission requirements evolve or as new devices are introduced. For the three PEDs used in this case study, weighting factors of 0.155, 0.265 and 0.580 were used for the Cellphone, GPS and Radio respectively after computing and normalising based on the respective PEDs battery capacities and utilisation/consumption patterns as was indicated in the previous section in Equations (11) and (12).

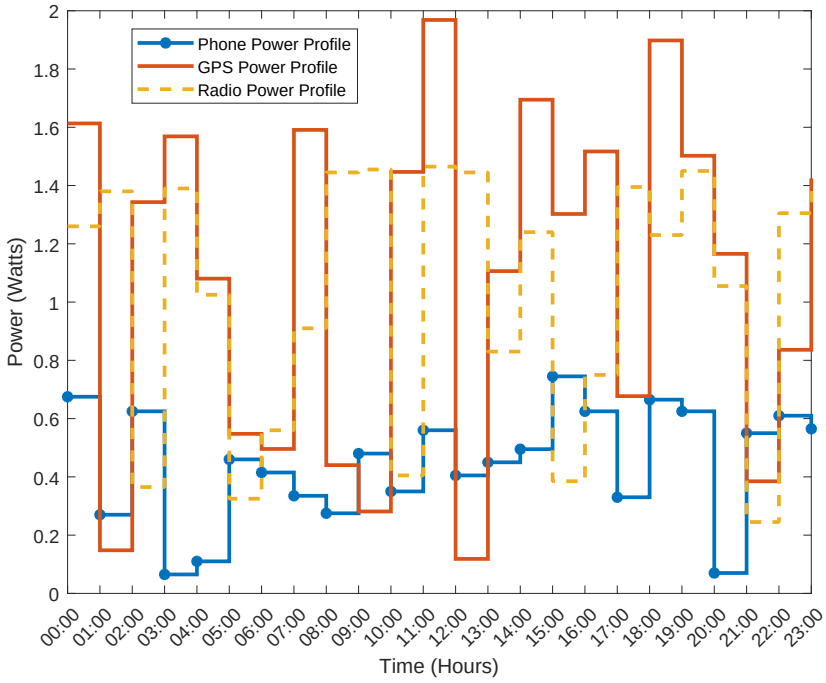

Figure 3. Portable electronic devices power profiles [23].

Table 2 gives the parameters used in this case study and their respective values. The charging times used in this study for both the main battery and the PEDs batteries are estimated benchmarks due to limited empirical data, offering baselines that may differ in practical settings. However, the primary emphasis remains on the model's functionality; the optimisation framework is designed to adapt to adjustments, ensuring continued optimal performance even if actual charging times deviate from these assumptions. In our previous study [23], we explored the impact of seasonal irradiance variability on solar optimisation, focusing on how changes in sunlight intensity affect system performance. This current study adds solar collector area as a variable, assessing its influence on optimisation in a way that effectively mirrors the impact of irradiance changes. Since both irradiance levels and collector area directly affect the total energy capture, varying either one achieves similar outcomes in terms of system performance. Increasing the collector area can compensate for lower irradiance levels during seasons with less sunlight, producing results comparable to those observed with increased irradiance in a smaller collector area. Therefore, treating both factors in the optimisation model is somewhat redundant, as either one alone provides sufficient insight into the system's adaptability to changes in solar availability. The model in this current study robustly adapts across diverse solar conditions without requiring simultaneous variation of both irradiance and collector area. This approach avoids redundancy while maintaining consistent optimisation.

Table 2. Case study parameters [23].

Parameter	Value
Charging efficiency (η_c)	0.9
Discharging efficiency (η_d)	0.95
Solar panel efficiency (η_{sol})	0.22
Solar PV area scenarios: (Ar)	0.025 m^2, 0.05 m^2 and 0.1 m^2
Depth of discharge (DOD)	0.95
Duration of one-time slot in minutes (T)	60 min
Duration of one time slot in hours (Δt)	$\frac{T}{60}$
Solar irradiance sampling time length (N)	24 h
The time it takes to fully charge the PED battery (α)	2 h
The time it takes to fully charge the main battery (ϕ)	3 h

5. Results and Discussion

Figure 4 shows the effect of solar collector area on main battery power flows. It illustrates how different solar collector areas ($0.025\ m^2, 0.05\ m^2$, and $0.1\ m^2$) impact the main battery's power flows in a system where solar PV is the sole source of battery charging, and the main battery subsequently discharges to the PEDs batteries. This analysis explores each subfigure in the context of the three scenarios, focusing on solar power output, power flow to the battery, and battery storage levels and SoC, offering a comparative understanding of how collector area influences these variables.

Subfigure (a) presents solar power output considering solar collector area scenarios. The power output generated by the solar panels over a 24-h period is shown for each scenario. The X-axis represents time in hours, while the Y-axis measures power in watts. The graph shows a distinct peak in power output around midday, reflecting typical sunlight intensity patterns. For Scenario 1 ($0.025\ m^2$), power output is modest, peaking at around 5 Watts, indicating a limited energy generation capacity due to the smaller collector area. Scenario 2 ($0.05\ m^2$) shows a moderate increase, with a peak power of approximately 10 Watts, while Scenario 3 ($0.1\ m^2$) achieves the highest peak of nearly 20 Watts. This trend demonstrates that a larger solar collector area captures more solar irradiance, thus producing more power. Consequently, Scenario 3 provides significantly more power across the daylight hours compared to the smaller areas, particularly during peak sunlight.

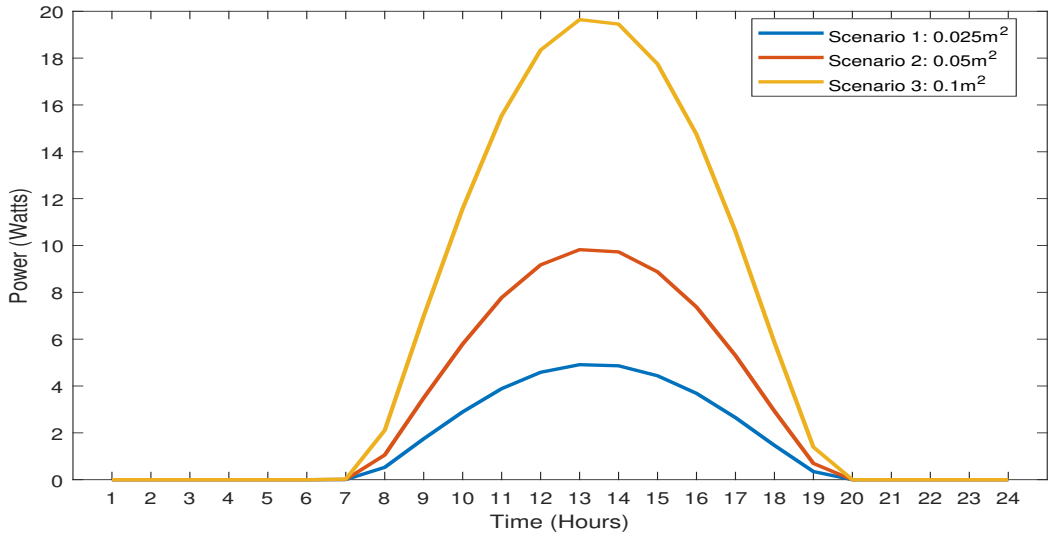

(**a**)

Figure 4. *Cont.*

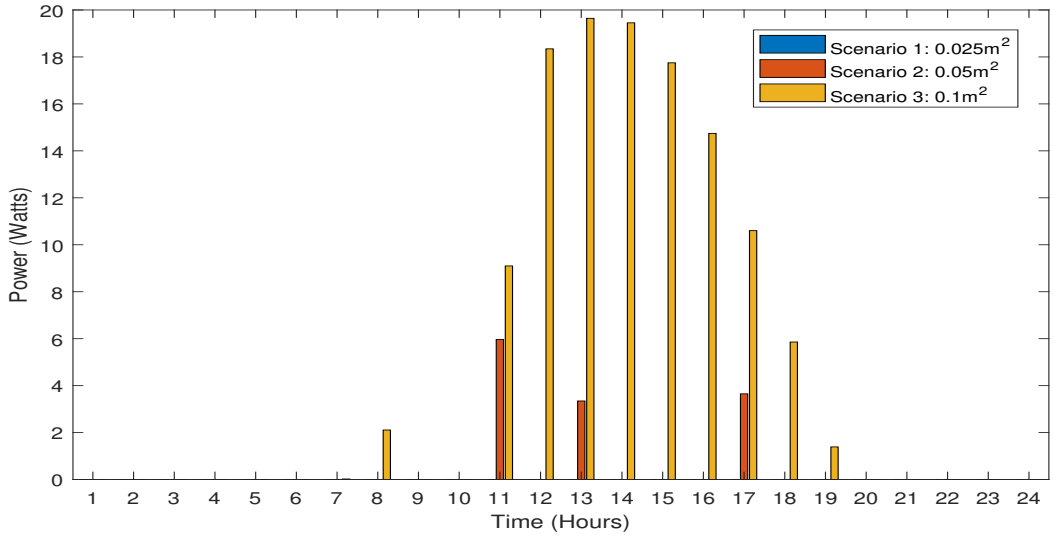

(**b**)

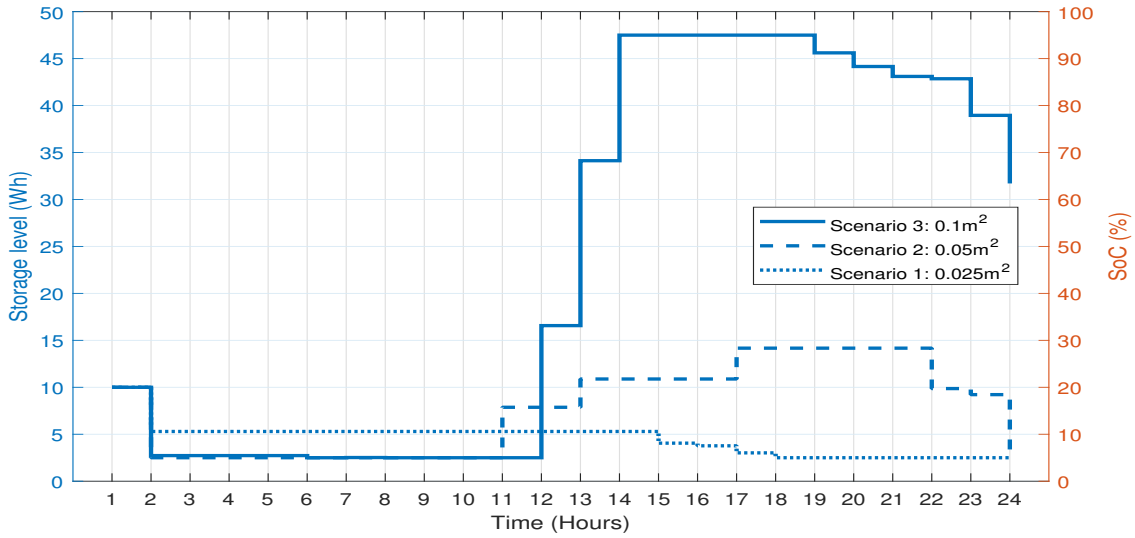

(**c**)

Figure 4. Effect of solar collector area on main battery power flows. (**a**) Solar power output considering solar collector area scenarios. (**b**) Solar PV to main battery power flows. (**c**) Main battery storage levels and State of charge.

Subfigure (b) presents solar PV to main battery power flows, illustrating the power transferred from the solar PV system to the main battery across the day. The X-axis again shows time in hours, and the Y-axis measures power in watts. This subfigure reveals how much and when power flows to the main battery for each scenario, effectively highlighting the charging duration and intensity. In Scenario 1, the smallest area, power flow to the main battery is limited and is almost zero. The small area restricts power availability, leading to inefficient charging of the main battery. Scenario 2 displays more robust power flow, with a peak of about 6 Watts, extending the charging duration slightly beyond Scenario 1. In Scenario 3, the largest area, the battery benefits from a broader and more powerful flow of energy, with peak power reaching 20 Watts and charging periods extending from early morning until late afternoon. Thus, larger collector areas not only increase the amount of power transferred to the main battery but also lengthen the daily charging period, enhancing the system's capacity to charge the battery consistently.

Subfigure (c) presents the main battery storage levels and State of charge, comparing the storage level and SoC of the main battery under each scenario. The X-axis shows time in hours, the left Y-axis represents storage level in watt-hours, and the right Y-axis shows SoC in percentage. This subfigure reflects the main battery's ability to store and maintain charge over the day as it receives energy from the solar PV system. In Scenario 1, with the smallest area, the battery's storage level remains consistently low, often below 5 Wh, with an unstable SoC that struggles to meet substantial power demands. This insufficient charging results from the limited power input from the small collector area. In Scenario 2, the SoC improves moderately, with storage levels reaching around 15 Wh and SoC peaking at approximately 30% during midday. While this scenario maintains a steadier SoC than Scenario 1, it still does not fully utilise the battery's potential storage capacity. Scenario 3, with the largest collector area, shows a substantial improvement, as the battery reaches nearly full capacity around midday, with storage levels peaking at 45–50 Wh and SoC approaching 100%. This high and stable SoC indicates that the battery can sustain demand more effectively, even during periods of lower irradiance.

Generally, as the solar collector area increases, we observe a proportional rise in solar power output, power flow to the battery, and battery storage levels. Scenario 3, with the largest area of 0.1 m^2, demonstrates the best performance, providing the highest and most consistent power flow to the main battery and enabling a stable, high SoC throughout the day. This scenario optimises the system's capacity to store and utilise solar energy, making it the most suitable choice for applications requiring reliable power storage. Conversely, Scenario 1, with the smallest area, is limited in its ability to charge the main battery effectively, resulting in low and unstable SoC levels that do not meet consistent demand. Scenario 2 offers a moderate improvement, but it still falls short of achieving the full storage potential seen in Scenario 3. This comparative analysis highlights the importance of a larger collector area in enhancing the main battery's power flows and energy storage efficiency, particularly in systems that rely solely on solar energy for charging. Scenarios 1 and 2 indicate the need for efficient charging prioritisation which is one of the major contributions of this study.

Further main battery dynamics are provided in Table 3. The table presents the power flows into and out of the main battery at every hour. The power flows to the main battery are denoted with positive sign while those going out to the PEDs are denoted with a negative sign and the power balance is shown in the last column. The charging and discharging behavior of the main battery is shaped by the optimisation and modelling approach that prioritises PED charging based on critical factors such as battery capacities, usage patterns, and operational priorities. This approach ensures that PED batteries—cellphone, GPS, and radio—receive power from the main battery in a way that aligns with their specific needs and the main battery's available energy therebgy maximising efficiency.

Solar PV is the sole source of incoming power to the main battery, and its availability fluctuates throughout the day. During peak sunlight hours, such as hour 11 (9.10 W), hour 12 (18.34 W), and hour 13 (19.64 W) , the main battery charges efficiently, creating a positive power balance as indicated by the fifth column of Table 3. These periods allow the main battery to store energy in anticipation of high-demand hours. The optimisation strategy leverages these peak periods to prioritise charging of the PEDs in alignment with their operational schedules, which helps maintain their functionality even when solar input decreases.

Discharge from the main battery to the PED batteries is managed according to each PED's requirements and the overall optimisation model. The respective PEDs battery charging are influenced by their respective battery status, usage patterns and operational criticality at any given hour. For example, the cellphone exhibits occasional high power demand, as seen in hour 15 with −13.00 W, likely due to prioritised usage during that hour. The GPS generally has low demand with minimal peaks (for instance, −0.12 W in hour 13). indicating efficient power management, possibly because it has lower operational priority at that particular hour. The radio, however, shows substantial intermittent demand,

particularly during hours 11 and 16 (−5.01 W and − 8.00 W, respectively), which could reflect critical operational requirements for communication or broadcasting functions that are prioritised by the optimisation model at those particular hours.

Table 3. Main battery power flows.

Hour	Power Flows from Solar PV to the Main Battery (W)	Power Flows from Main Battery to Cellphone Battery (W)	Power Flows from Main Battery to GPS Battery (W)	Power Flows from Main Battery to Radio Battery (W)	Main Battery Power Balance (W)
1	0.00	−2.88	−4.79	−2.66	−10.33
2	0.00	0.00	−2.39	−5.27	−7.65
3	0.00	0.00	0.00	0.00	0.00
4	0.00	0.00	0.00	0.00	0.00
5	0.00	0.00	0.00	0.00	0.00
6	0.00	−0.24	0.00	0.00	−0.24
7	0.02	0.00	0.00	0.00	0.02
8	2.11	0.00	−2.02	0.00	0.09
9	0.00	0.00	0.00	0.00	0.00
10	0.00	0.00	0.00	0.00	0.00
11	9.10	0.00	−3.60	−5.01	0.48
12	18.34	−1.49	0.00	−1.08	15.77
13	19.64	0.00	−0.12	0.00	19.52
14	19.45	0.00	−4.35	0.00	15.10
15	17.45	−13.00	−3.81	0.00	0.93
16	14.74	0.00	−5.97	−8.00	0.78
17	10.60	0.00	−10.04	0.00	0.56
18	5.86	−2.32	−0.97	−2.26	0.31
19	1.39	0.00	−2.00	−1.30	−1.91
20	0.00	0.00	0.00	−1.53	−1.53
21	0.00	0.00	0.00	−1.11	−1.11
22	0.00	0.00	0.00	−0.26	−0.26
23	0.00	0.00	−4.10	0.00	−4.10
24	0.00	−3.26	−1.50	−2.87	−7.63

The optimisation model effectively manages the different demands by charging PEDs during high solar input hours and using stored energy when solar power is insufficient. The main battery has a capacity of 50 W and a depth of discharge (DoD) of 95%, allowing it to discharge up to 47.5 W. This substantial discharge limit enables the main battery to support PEDs even during hours of low solar input. However, when PED demand is high and solar input is low, the model prioritises the most critical needs, as seen in hour 15 when the main battery balance reaches 0.93 W due to significant power draw from the cellphone. This prioritisation ensures that essential PED functions remain operational, even if it temporarily reduces the main battery's charge. The optimisation model allocates power to PEDs based on priority, which helps avoid excessive depletion of the main battery and prevents complete discharge that could disrupt operations.

To summarise the results presented in Table 3, the optimisation and modelling approach allows for a dynamic charging and discharging cycle that accommodates both the variability of solar energy and the distinct requirements of each PED. By prioritising critical functions and aligning with battery statuses and usage patterns, the system sustains PED operation efficiently. Overall, if the power flows from the main battery to each respective PED battery are summed separately, it can be deduced from Table 3 that the system prioritises charging of the GPS, followed by the radio and lastly the cellphone. While this approach effectively balances charging during peak solar periods and discharging during high-demand hours, prolonged low solar conditions combined with sustained high PED demands could still challenge the main battery's capacity, highlighting the importance of this study and moreso the need for similar careful prioritisation in off-grid power systems.

Figure 5 illustrates the discharging power flows of batteries for PEDs, specifically for the cellphone, GPS devices, and radio, across three scenarios with varying solar collector areas. Each scenario represents a different solar collector area: Scenario 1 with 0.025 m^2, Scenario 2 with 0.05 m^2, and Scenario 3 with 0.1 m^2. The y-axis in each subfigure shows the power (in watts) discharged by each PED battery to its respective electronics, while the x-axis covers a 24-h period, showing time in hours. The colors correspond to different PEDs: blue for cellphone battery discharge, brown for GPS battery discharge, and green for radio battery discharge. Importantly, in all scenarios, only the PED batteries power the PED electronics; neither the main battery nor the solar PV system directly supplies power to the PED electronics.

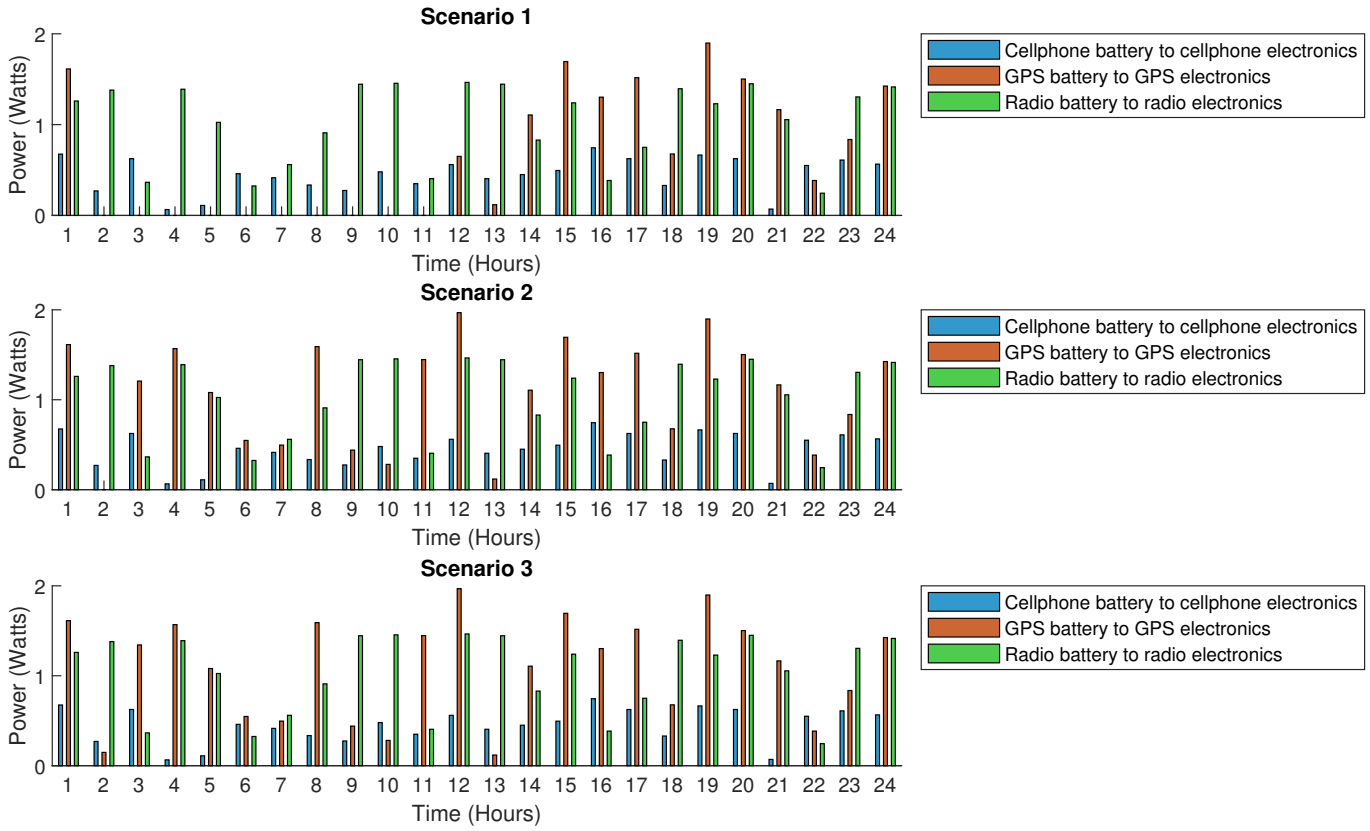

Figure 5. Effect of solar collector area on PED batteries discharging power flows.

In Scenario 1, the smallest solar collector area (0.025 m^2) results in frequent and relatively high peaks in discharging power flows across all PEDs. This scenario is analogous to a low solar irradiance condition, where insufficient solar energy is available to support or recharge the PED batteries effectively. Consequently, the batteries discharge more frequently and at higher intensities to meet the power demands of the electronics. For instance, the cellphone battery shows numerous spikes throughout the day, indicating frequent power demand that the battery has to fulfill due to limited solar energy support. Similarly, the GPS battery experiences moderate but fluctuating peaks, while the radio battery discharges consistently, but with lower peak power requirements. Overall, Scenario 1 demonstrates that a small solar collector area leads to high dependency on battery discharge due to insufficient solar energy input.

Moving to Scenario 2, which doubles the solar collector area to 0.05 m^2, there is a noticeable reduction in both the frequency and intensity of battery discharges across all PEDs. This scenario corresponds to a moderate irradiance level, where increased solar energy support alleviates some of the discharge burden on the PED batteries. The cellphone battery's discharge profile shows fewer and less intense peaks compared to Scenario 1,

indicating that the additional solar energy reduces the battery's need to power the cellphone electronics continuously. The GPS battery also benefits, with fewer discharge fluctuations and lower peak power levels, while the radio battery shows a smoother discharge profile, suggesting that the solar collector area is now providing a more stable supplementary energy source. Scenario 2 highlights that a moderate increase in solar collector area can significantly reduce the load on PED batteries by supplying some of the necessary energy directly to the electronics.

In Scenario 3, with the largest solar collector area of 0.1 m^2, the impact of increased solar energy support is even more pronounced. This scenario is analogous to a high irradiance condition, where solar energy input is substantial enough to meet a significant portion of the PED electronics' power demands, minimising the need for battery discharge. The cellphone battery discharges infrequently, with very low peak power levels, indicating that the large solar collector area is almost sufficient to sustain the cellphone electronics. Similarly, the GPS battery exhibits minimal discharges, with few fluctuations and reduced peak levels, suggesting that the higher solar input is meeting the GPS device's power needs more effectively. The radio battery's discharge profile in this scenario is notably flat, with barely any peaks, indicating that the radio electronics are largely supported by solar energy without relying heavily on battery power. Scenario 3 demonstrates that with a large solar collector area, PED batteries experience minimal discharge, as the solar energy input is adequate to meet most, if not all, of the power needs of the electronics.

Overall, Figure 5 reveals a clear trend in the effect of solar collector area on PED battery discharge patterns. Scenario 1 shows high and frequent discharges, indicative of low irradiance and limited solar support. Scenario 2 reduces discharge frequency and intensity, reflecting moderate irradiance, while Scenario 3 minimises discharge, with solar energy meeting most of the power demands, indicative of high irradiance. Increasing the solar collector area effectively reduces the load on PED batteries by supplying a greater share of the power required by the electronics, thus extending battery life and ensuring a stable power flow to the devices. This analysis shows the importance of solar collector area in supporting PEDs operations and reducing reliance on battery power, particularly in conditions where continuous use is necessary.

Figure 6 demonstrates the impact of varying solar collector areas on the power flows for charging PEDs (cellphone, GPS and radio) batteries. Each scenario corresponds to a different solar collector area size—Scenario 1 with a collector area of 0.025 m^2, Scenario 2 with 0.05 m^2, and Scenario 3 with 0.1 m^2—reflecting an increase in available solar energy or irradiance. The subfigures illustrate hourly power flows (in watts) directed towards each PED battery from either solar PV or main battery sources over a 24-h period. The x-axis shows time in hours, while the y-axis indicates power levels, capturing the intensity and timing of power flows throughout the day.

In Scenario 1, with the smallest collector area of 0.025 m^2, solar energy availability is limited, resulting in low power flows from the solar source to the PED batteries. The power contributions from solar sources barely exceed 5 watts, even during peak midday hours, which restricts the charging capacity for devices. This limited solar energy mostly supports charging the cellphone and GPS batteries, while the radio battery, in particular, relies more heavily on the main battery. Most charging occurs between hour 10 a.m. and 4 p.m., with minimal or no power flows outside of these midday hours, reflecting the reduced effectiveness of solar charging with such a small collector area. The main battery thus plays a crucial role in supplementing the charging needs, especially for the radio, underscoring the limited contribution of solar power under this scenario.

Scenario 2, with a doubled solar collector area to that of scenario 1, sees a marked improvement in solar energy availability, which allows for higher power flows directed towards PED batteries. Here, the solar contribution reaches around 10 watts during peak hours, providing a more substantial charging capacity for the GPS and cellphone batteries. The radio battery also benefits more from solar power in this scenario, though it still leans on the main battery at certain times, particularly in early morning and late evening hours.

Solar charging duration extends across more of the daylight hours, from around 8 a.m. to 4 p.m., allowing for a more continuous flow of solar energy compared to Scenario 1. This reduces the main battery's load, particularly for GPS and cellphone charging, as the increased solar power sustains charging for a more extended portion of the day.

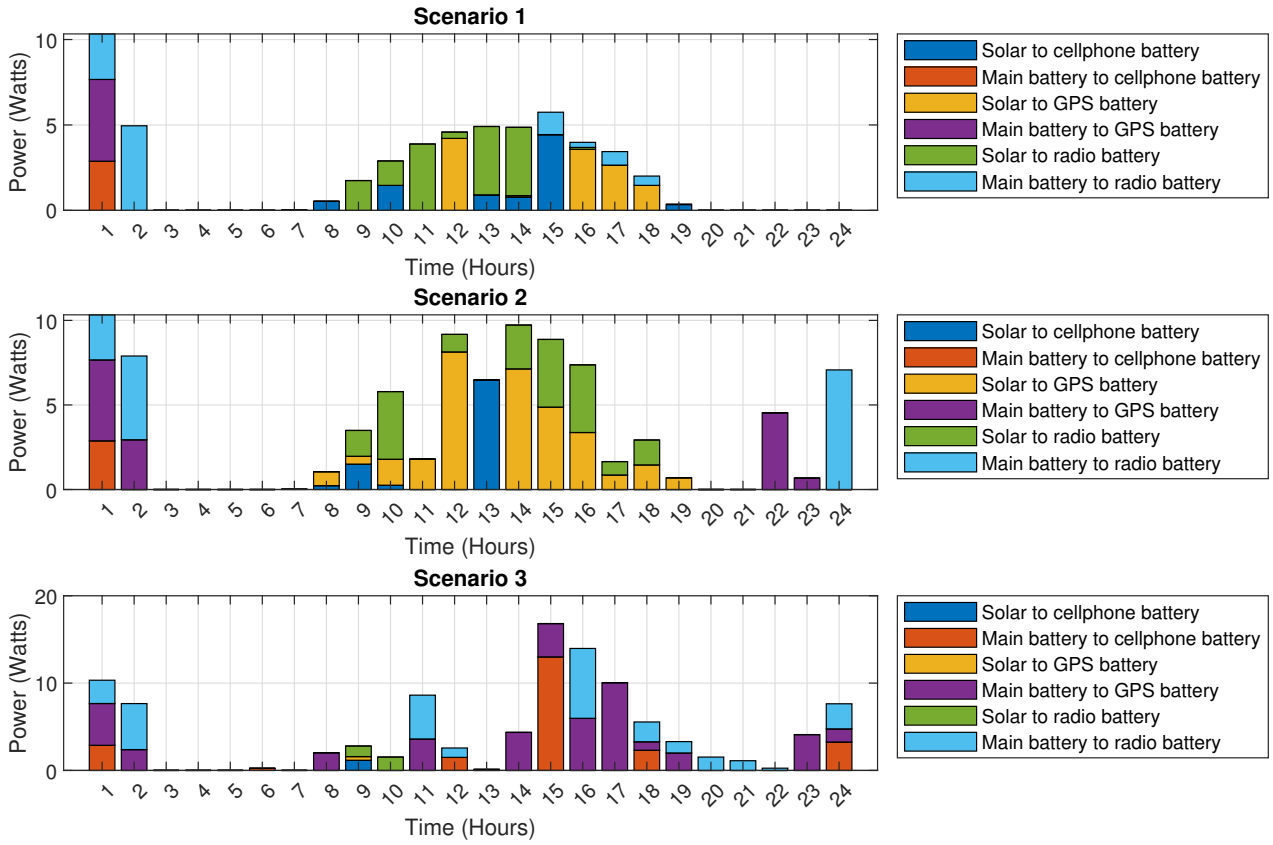

Figure 6. Effect of solar collector area on PED batteries charging power flows.

In Scenario 3, where the solar collector area is the largest at 0.1 m^2, solar power availability peaks, enabling the highest power flows of up to 18 watts. This significant increase allows the PED batteries, especially the GPS and cellphone, to receive a much larger share of solar power. The charging of PEDs is sustained much longer into the morning and evening hours compared to the previous scenarios, illustrating the impact of a larger collector area on extending the effective charging period.

Comparing the three scenarios, it is clear that increasing the solar collector area significantly enhances both the intensity and duration of solar power availability. Scenario 1's small collector area leads to limited and intermittent charging. Scenario 2 shows an improvement in solar charging duration and intensity, reducing but not eliminating the need for the main battery. Scenario 3, with the largest collector area, results in the most sustained PEDs battery charging. This trend points out to the positive impact of larger collector areas on PED charging efficiency, suggesting that optimising the collector size can improve power sustainability, especially in scenarios with limited energy resources.

Figure 7 presents a comparative analysis of the effect of three different solar collector areas on the storage levels of batteries powering three types of PEDs (cellphone, GPS and radio). Since the solar collector area is directly related to the amount of solar irradiance captured, each increase in area allows for more energy to be harvested and stored, influencing the batteries' state of charge over a 24-h period.

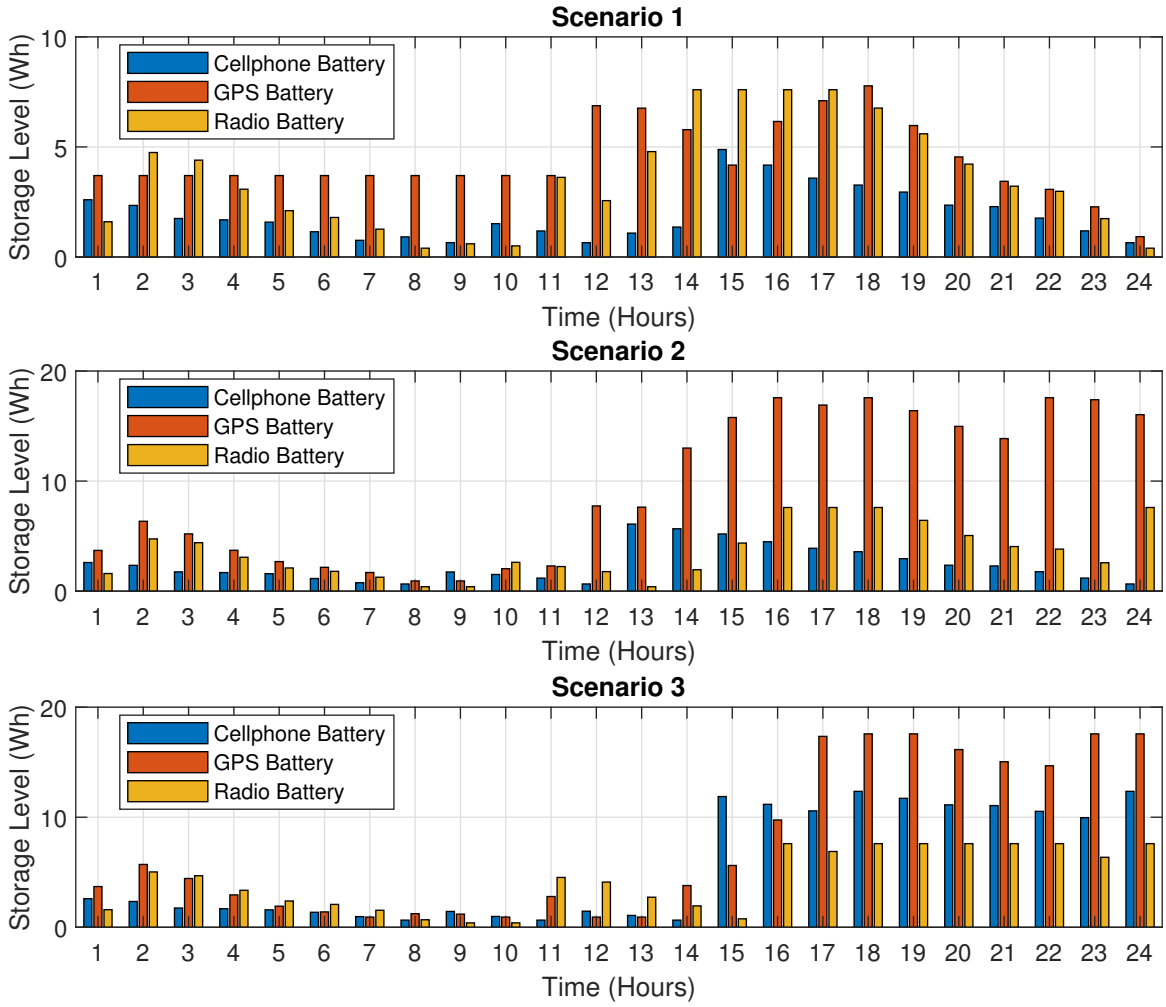

Figure 7. Effect of solar collector area on PED batteries storage levels.

In Scenario 1, the smallest collector area of 0.025 m^2 results in limited energy input, as seen in the relatively low storage levels across all three PED batteries. Storage peaks occur during midday, around hours 12 to 17, when solar irradiance is expected to be highest. Even during these peak hours, however, none of the batteries exceed a storage level of 10 Wh. The GPS battery achieves the highest storage level among the three, followed by the radio battery and, finally, the cellphone battery, which has the lowest storage level. The limited solar collector area restricts the energy available to all devices, resulting in low storage levels and a correspondingly lower SoC throughout the day.

In Scenario 2, doubling the solar collector area to 0.05 m^2 results in a marked improvement in battery storage levels. The PEDs can now store more energy, with peak storage levels approaching 18 Wh for the GPS battery and moderate increases in the cellphone and radio batteries compared to Scenario 1. The energy storage builds up steadily over the morning hours, with a more pronounced and sustained peak in the afternoon and evening, indicating an extended period of adequate charging due to the increased solar collector area. As in Scenario 1, the GPS battery reaches the highest state of charge among the devices, highlighting the GPS's criticality over other devices. This scenario demonstrates that a moderate increase in solar collector area significantly enhances the energy available to each PED, supporting a higher state of charge, particularly during hours of high irradiance.

In Scenario 3, the solar collector area is increased further to 0.1 m^2, providing the highest energy input to the PEDs. This larger area results in substantial improvements in storage levels across all devices far above those in previous scenarios. The increased energy input allows the batteries to maintain higher levels throughout the day, even during

early morning and evening hours when solar irradiance is lower. This scenario indicates the benefits of a larger solar collector area, as it enables each PED to capture more solar energy, achieve a higher state of charge, and sustain storage levels for a prolonged period. The broader and more prolonged peaks in storage levels across devices demonstrate how increased irradiance from a larger collector area supports continuous and robust battery charging.

Comparatively, across all three scenarios, the effect of increasing the solar collector area is clear: higher energy input enables greater battery storage and higher states of charge for each PED. The cellphone battery consistently exhibits the lowest storage levels, suggesting it has lower energy requirements than the GPS and radio batteries. The radio battery displays intermediate storage levels, indicating it benefits from the increased collector area but to a lesser extent than the GPS battery. The GPS battery consistently shows the highest storage levels across scenarios, implying that its charging is prioritised, allowing it to reach a higher SoC. These findings show that optimising solar collector area is essential for enhancing the energy autonomy of PEDs, with larger areas significantly extending battery life and operational capacity.

In light of the battery levels and utilisation considerations, the charging prioritisation objective in this study seeks to optimise the distribution of available charging resources to maximise operational effectiveness. Scenario 3, of solar collector area 0.1 m^2 is used to elaborate on the optimisation and charging prioritisation results obtained for the three PEDs used in the case study. To maximise the sum of battery level (SoC) and utilisation across all devices, the optimisation process yields a distinct charging prioritisation scheme as presented in Figures 8–10.

The highest charging priority is accorded to the GPS, aligning with its critical role and high utilisation demands. Ensuring the GPS remains adequately charged is deemed imperative to sustain crucial navigation and positioning functionalities, especially in demanding environments where reliable location data is indispensable. Prioritising the charging of the GPS over the radio and cellphone is imperative for uninterrupted operations of these critical devices. The GPS serves as a critical tool for precise navigation and orientation. Its unavailability due to loss of battery power could compromise the realisation of intended tasks. While communication is vital, the consequences of losing GPS functionality outweigh the temporary loss of cellphone and radio communication. Furthermore, in emergencies, the GPS provides accurate location data for timely assistance or evacuation, potentially saving lives. By prioritising GPS charging, its availability is ensured thereby reducing dependency on external factors and maintaining operational readiness. Thus, while communication is essential, the unique capabilities of the GPS make it the top priority for charging, safeguarding mission effectiveness and personnel safety.

Following closely, the Radio is assigned the second-highest priority for charging. While not as power-intensive as the GPS, the Radio's significance in enabling communication and information dissemination warrants a substantial allocation of charging resources. This prioritisation decision reflects the acknowledgment of the Radio's pivotal role in facilitating real-time communication among deployed units, enhancing situational awareness, and supporting tactical decision-making processes. While communication is vital for coordination and intelligence sharing, the GPS takes precedence due to its provision of essential location data, ensuring precise navigation and orientation crucial for mission success and personnel safety, particularly in unfamiliar or hostile environments. However, the radio's capability to establish communication is indispensable for effective teamwork and operational coordination. While the loss of radio communication might impede coordination, its temporary unavailability is considered less detrimental than losing GPS functionality. Therefore prioritising the radio as the second charging priority device guarantees maintenance of communication capabilities while acknowledging the paramount importance of accurate navigation provided by the GPS for mission success and personnel safety.

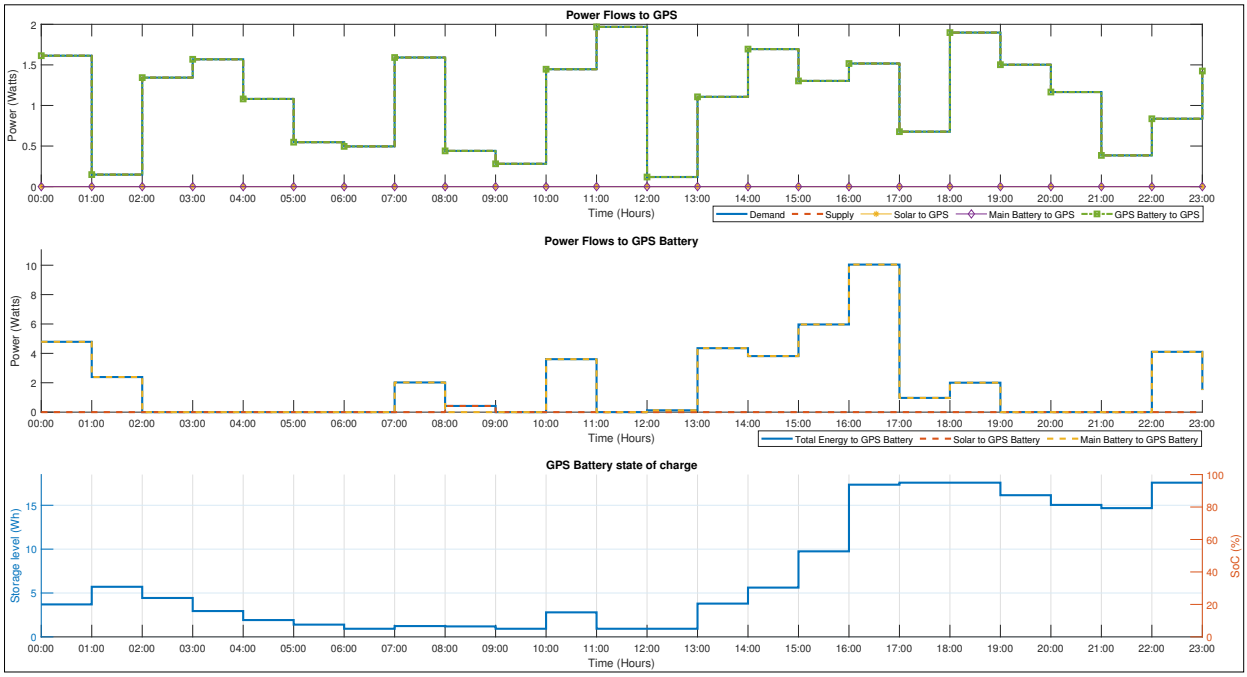

Figure 8. Power flows to GPS electronics, GPS battery and GPS battery state of charge.

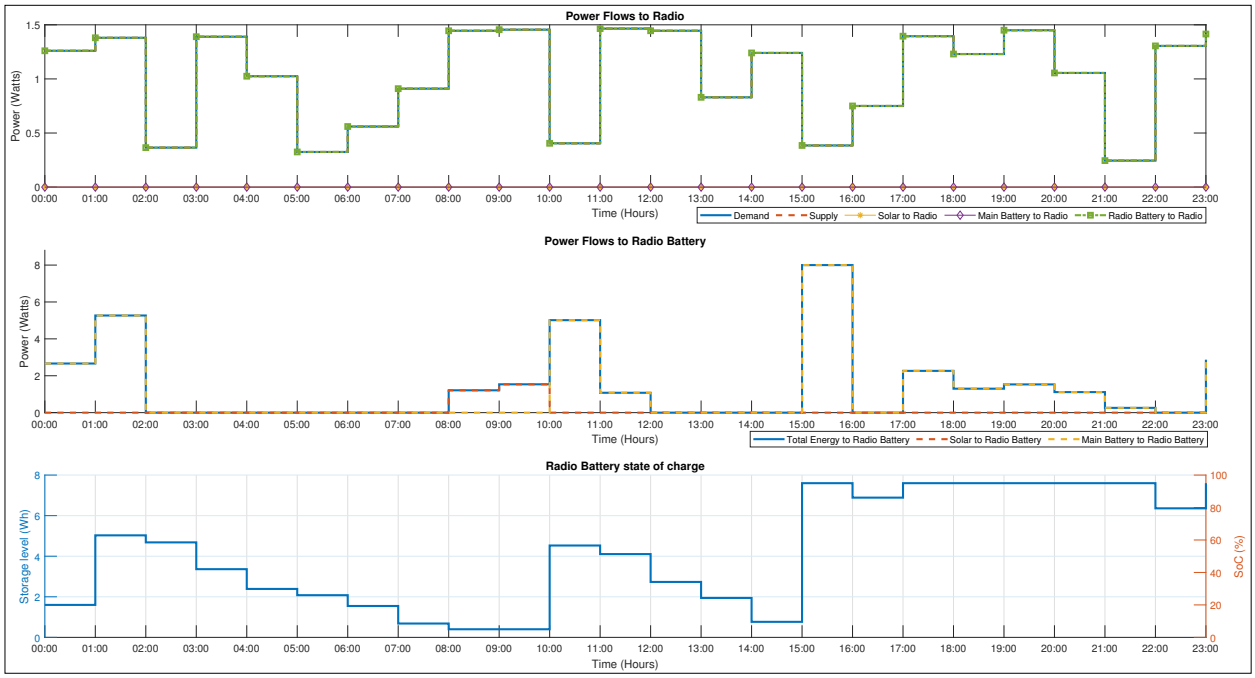

Figure 9. Power flows to radio electronics, radio battery and radio battery state of charge.

Conversely, the Cellphone assumes the lowest priority for charging, despite its moderate battery capacity. This decision is informed by its comparatively lower utilisation and perceived non-essential functionalities in the context of immediate operational requirements. While the Cellphone may serve ancillary purposes such as data communication, reconnaissance, or logistical support, its charging priority is deemed secondary to the critical operational demands addressed by the GPS and Radio. The cellphone's dependency on network coverage leaves it vulnerable to disruptions like outages or jamming, making it less dependable during critical operations compared to the radio. Moreover, the GPS holds precedence over the cellphone as it provides crucial location data essential for accurate

navigation and orientation, crucial for mission success and personnel safety, especially in hostile environments. In emergencies, the GPS facilitates precise location identification for timely aid or evacuation, potentially saving lives. By prioritising GPS charging, its availability for future missions is ensured, reducing reliance on external factors and maintaining operational readiness. Thus, while communication is vital, the GPS's unique capabilities make it the top priority for charging, followed by the radio, while the cellphone, reliant on external networks, is assigned the lowest charging priority in the optimisation context given.

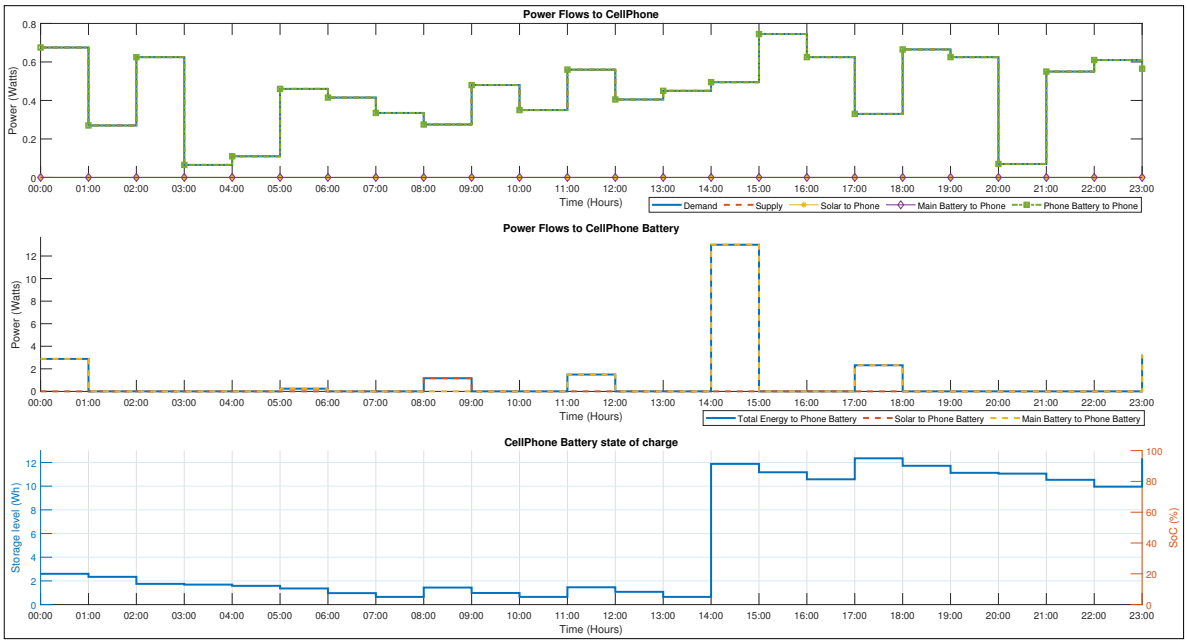

Figure 10. Power flows to Cellphone electronics, Cellphone battery and Cellphone battery state of charge.

Thus, by strategically allocating charging priorities based on a holistic assessment of battery capacities, utilisation patterns, and operational imperatives, the optimisation process aimed to enhance overall task effectiveness and device readiness in a dynamic and resource-constrained environment. In summary, the findings from this study contribute to a growing body of research on energy management and charging prioritisation for PEDs. By considering factors such as battery capacities, utilisation patterns, and operational imperatives, the optimisation process enhances readiness and operational efficiency in a limited charging resource scenario. These findings build upon and corroborate previous research works, highlighting the importance of strategic energy management in supporting task success in diverse operational contexts.

In a broader context encompassing any number of PEDs with varying battery capacities and distinct utilisation or demand profiles, the principles underlying charging prioritisation remain consistent, albeit with adjustments to accommodate the specific characteristics of each device. The optimisation process hinges on striking a delicate balance between the storage capacity of each device and its corresponding power demands during operation. Regardless of the number of devices involved, the overarching objective remains centered on maximising operational efficiency by judiciously allocating charging resources to address critical operational needs. This entails prioritising devices with higher utilisation or demand profiles and ensuring their sustained functionality through timely recharging. Moreover, the optimisation process may dynamically adapt to fluctuations in operational requirements, reallocating charging priorities as needed to optimise resource utilisation and enhance mission effectiveness. Consequently, while the specifics of charging prioritisation may vary based on the composition and characteristics of the PEDs in question, the fun-

damental objective of optimising energy distribution to support operational objectives remains paramount across diverse scenarios and deployments.

6. Conclusions

This study demonstrates the effectiveness of a simulation-based approach to optimise charging prioritisation for solar PV-powered portable electronic devices (PEDs), incorporating critical factors like battery capacities, usage patterns, operational priorities, and solar collector area. By introducing solar collector area as a variable, this research analyses its impact on charging prioritisation similarly to irradiance variability, as both influence solar energy capture. Adjusting the collector area serves as a compensatory mechanism for reduced irradiance during off-peak seasons, with findings showing that a larger collector area of 0.1 m^2 significantly enhances charging efficiency and device functionality by ensuring stable or increasing battery levels. In contrast, smaller collector areas $(0.025\ m^2)$ and 0.05 m^2) struggle to maintain sufficient charge, with the smallest area resulting in rapid battery decline due to intermittent charging. In such cases where the primary energy resource is limited, the optimisation approach prioritises devices with high criticalities, such as GPS units, to ensure continuous functionality of the same.

By dynamically adjusting priorities based on real-time demand, energy distribution efficiency is enhanced and device readiness and task execution are improved, particularly in resource-limited environments. The robust modelling approach, which integrates battery status, operational needs, and collector area, establishes a scalable framework adaptable to diverse operational scenarios. These findings emphasise the potential of intelligent charging systems to support sustainable, resilient energy management for PEDs, providing valuable insights into energy-efficient device operation and resource allocation under challenging conditions. This work distinguishes from previous research by offering practical guidance for optimising energy distribution to support operational needs and extend device lifespan. Overall, limitations of typical commercial PV-driven systems, which often rely on uniform or first-come, first-served charging without considering device criticality, real-time usage, or battery status are overcame. Future work is envisioned to explore predictive modelling for real-time adaptation, potentially integrating model predictive control approaches among other artificial intelligence-driven forecasts to more accurately anticipate usage and charging needs.

Author Contributions: Conceptualization, T.K., H.C.M. and A.D.F.; data curation, T.K.; funding acquisition, H.C.M.; investigation, T.K.; methodology, T.K., H.C.M. and A.D.F.; project administration, H.C.M. and A.D.F.; resources, H.C.M.; supervision, H.C.M.; writing—original draft, T.K.; writing—review and editing, T.K., H.C.M. and A.D.F. All authors have read and agreed to the published version of the manuscript.

Funding: Research was sponsored by the ARO and was accomplished under Grant Number: W911NF-22-1-0006. The views and conclusions contained in this document are those of the authors and should not be interpreted as representing the official policies, either expressed or implied, of ARO or the U.S. Government. The U.S. Government is authorized to reproduce and distribute reprints for Government purposes notwithstanding any copyright notation herein.

Data Availability Statement: Publicly available meteorological datasets from the Southern African Universities Radiometric Network (SAURAN) were used in this study. These data can be found here: https://sauran.ac.za/ (accessed on 4 March 2024).

Conflicts of Interest: The authors declare no conflicts of interest.

References

1. Dion, H.; Evans, M. Strategic frameworks for sustainability and corporate governance in healthcare facilities; approaches to energy-efficient hospital management. *Benchmarking Int. J.* **2024**, *31*, 353–390. [CrossRef]
2. Kaygusuz, K. Energy for sustainable development: A case of developing countries. *Renew. Sustain. Energy Rev.* **2012**, *16*, 1116–1126. [CrossRef]

3. Samaras, C.; Nuttall, W.J.; Bazilian, M. Energy and the military: Convergence of security, economic, and environmental decision-making. *Energy Strategy Rev.* **2019**, *26*, 100409. [CrossRef]
4. Burns, M.G. *Managing Energy Security: An All Hazards Approach to Critical Infrastructure*; Routledge: London, UK, 2019.
5. Ukoba, K.; Yoro, K.O.; Eterigho-Ikelegbe, O.; Ibegbulam, C.; Jen, T. Adaptation of solar power in the Global south: Prospects, challenges and opportunities. *Heliyon* **2024**, *10*, e28009
6. Maxmut, O.; Xamitov, F. Renewable energy sources: Advancements, challenges, and prospects. *Int. J. Adv. Sci. Res.* **2023**, *3*, 14–25.
7. Streimikiene, D.; Kyriakopoulos, G. Energy poverty and low carbon energy transition. *Energies* **2023**, *16*, 610. [CrossRef]
8. Hasan, M.; Hossain, S.; Mofijur, M.; Kabir, Z.; Badruddin, I.A.; Yunus, K.; Jassim, E. Harnessing solar power: A review of photovoltaic innovations, solar thermal systems, and the dawn of energy storage solutions. *Energies* **2023**, *16*, 6456. [CrossRef]
9. Sun, J.; Xie, Y.; Zhou, S.; Dan, J. The role of solar energy in achieving net-zero emission and green growth: A global analysis. *Econ. Chang. Restruct.* **2024**, *57*, 46. [CrossRef]
10. Ebhota, W.S.; Jen, T.C. Fossil fuels environmental challenges and the role of solar photovoltaic technology advances in fast tracking hybrid renewable energy system. *Int. J. Precis. Eng. Manuf.-Green Technol.* **2020**, *7*, 97–117. [CrossRef]
11. El Hammoumi, A.; Chtita, S.; Motahhir, S.; El Ghzizal, A. Solar PV energy: From material to use, and the most commonly used techniques to maximize the power output of PV systems: A focus on solar trackers and floating solar panels. *Energy Rep.* **2022**, *8*, 11992–12010. [CrossRef]
12. Malinowski, M.; Leon, J.I.; Abu-Rub, H. Photovoltaic energy systems. In *Power Electronics in Renewable Energy Systems and Smart 727 Grid: Technology and Applications*; Wiley Online Library: New York, NY, USA, 2019; pp. 347–389.
13. Ostfeld, A.E.; Arias, A.C. Flexible photovoltaic power systems: Integration opportunities, challenges and advances. *Flex. Print. Electron.* **2017**, *2*, 013001. [CrossRef]
14. Teichert, O.; Chang, F.; Ongel, A.; Lienkamp, M. Joint optimization of vehicle battery pack capacity and charging infrastructure for electrified public bus systems. *IEEE Trans. Transp. Electrif.* **2019**, *5*, 672–682. [CrossRef]
15. Li, L.; Wu, J.; Xu, Y.; Che, J.; Liang, J. Energy-controlled optimization algorithm for rechargeable unmanned aerial vehicle network. In Proceedings of the 2017 12th IEEE Conference on Industrial Electronics and Applications (ICIEA), Siem Reap, Cambodia, 18–20 June 2017; IEEE: New York, NY, USA, 2017; pp. 1337–1342.
16. Mohsan, S.A.H.; Khan, M.A.; Noor, F.; Ullah, I.; Alsharif, M.H. Towards the unmanned aerial vehicles (UAVs): A comprehensive review. *Drones* **2022**, *6*, 147. [CrossRef]
17. Saatloo, A.M.; Mehrabi, A.; Marzband, M.; Aslam, N. Hierarchical user-driven trajectory planning and charging scheduling of autonomous electric vehicles. *IEEE Trans. Transp. Electrif.* **2022**, *9*, 1736–1749. [CrossRef]
18. Thantharate, P.; Thantharate, A.; Kulkarni, A. GREENSKY: A fair energy-aware optimization model for UAVs in next-generation wireless networks. *Green Energy Intell. Transp.* **2024**, *3*, 100130. [CrossRef]
19. Pakrooh, R.; Bohlooli, A. A survey on unmanned aerial vehicles-assisted internet of things: A service-oriented classification. *Wirel. Pers. Commun.* **2021**, *119*, 1541–1575. [CrossRef]
20. Hejres, S.; Mahjoub, A.; Hewahi, N. Routing Approaches used for Electrical Vehicles Navigation: A Survey. *Int. J. Comput. Digit. Syst.* **2024**, *15*, 801–819. [CrossRef]
21. Zhang, J.; Jing, W.; Lu, Z.; Wu, H.; Wen, X. Collaborative strategy for electric vehicle charging scheduling and route planning. In *IET Smart Grid*; Wiley Online Library: New York, NY, USA, 2024.
22. Kovačević, I.F.; Kolar, J.W.; Round, S.D.; Vasić, M. Mission Profile Based Optimization of a Wearable Power System. *EPE J.* **2013**, *23*, 36–47. [CrossRef]
23. Kunatsa, T.; Myburgh, H.C.; De Freitas, A. Optimal Power Flow Management for a Solar PV-Powered Soldier-Level Pico-Grid. *Energies* **2024**, *17*, 459. [CrossRef]
24. Alsabbagh, A.; Yin, H.; Ma, C. Distributed charging management of multi-class electric vehicles with different charging priorities. *IET Gener. Transm. Distrib.* **2019**, *13*, 5257–5264. [CrossRef]
25. Jayachandran, M.; Rao, K.P.; Gatla, R.K.; Kalaivani, C.; Kalaiarasy, C.; Logasabarirajan, C. Operational concerns and solutions in smart electricity distribution systems. *Util. Policy* **2022**, *74*, 101329. [CrossRef]
26. Saldaña, G.; San Martin, J.I.; Zamora, I.; Asensio, F.J.; Oñederra, O. Electric vehicle into the grid: Charging methodologies aimed at providing ancillary services considering battery degradation. *Energies* **2019**, *12*, 2443. [CrossRef]
27. Abdullah, H.M.; Gastli, A.; Ben-Brahim, L. Reinforcement learning based EV charging management systems—A review. *IEEE Access* **2021**, *9*, 41506–41531. [CrossRef]
28. Brown, E.M.; Potter, L.A. Army Futures Command Concept for Intelligence 2028. U.S. Army Technical Report: AFC Pam 71-20-3. 2020. Available online: https://apps.dtic.mil/sti/pdfs/AD1128558.pdf (accessed on 28 August 2024).
29. Celik, B.; Roche, R.; Suryanarayanan, S.; Bouquain, D.; Miraoui, A. Electric energy management in residential areas through coordination of multiple smart homes. *Renew. Sustain. Energy Rev.* **2017**, *80*, 260–275. [CrossRef]
30. Karakoç, T.H.; Ekici, S.; Dalkiran, A. *Life Cycle Assessment in Aviation: Theory and Applications*; Springer Nature: Berlin/Heidelberg, Germany, 2024.
31. Teixeira, K.; Miguel, G.; Silva, H.S.; Madeiro, F. A Survey on Applications of Unmanned Aerial Vehicles using Machine Learning. *IEEE Access* **2023**, *11*, 117582–117621. [CrossRef]

32. Roege, P.E.; Schihl, P.; Kirker, R.; Army Training and Doctrine Command Fort Monroe va Army Capabilities Integration Center. Power and energy strategy white paper. In *Fort Monroe: Army Capabilities Integration Center-Research, Development and Engineering Command-Deputy Chief of Staff, G-4*; Army Training and Doctrine Command Fort Monroe va Army Capabilities Integration Center: Washington, DC, USA, 2010.
33. Borges, N.P.; Ghedini, C.G.; Ribeiro, C.H.C. Safe path prioritization for multi-unit visiting missions performed by UAVs. *Res. Sq.* 2024, *preprint*. [CrossRef]
34. Xia, X.; Zhang, J. Operation efficiency optimisation modelling and application of model predictive control. *IEEE/CAA J. Autom. Sin.* **2015**, *2*, 166–172. [CrossRef]
35. Tazvinga, H.; Xia, X.; Zhang, J. Minimum cost solution of photovoltaic–diesel–battery hybrid power systems for remote consumers. *Sol. Energy* **2013**, *96*, 292–299. [CrossRef]
36. Abdalla, A.A.; El Moursi, M.S.; El-Fouly, T.H.; Al Hosani, K.H. Reliant Monotonic Charging Controllers for Parallel-Connected Battery Storage Units to Reduce PV Power Ramp Rate and Battery Aging. *IEEE Trans. Smart Grid* **2023**, *14*, 4424–4438. [CrossRef]
37. Bestuzheva, K.; Chmiela, A.; Müller, B.; Serrano, F.; Vigerske, S.; Wegscheider, F. Global optimization of mixed-integer nonlinear programs with SCIP 8. *J. Glob. Optim.* **2023**, 1–24. [CrossRef]
38. Berthold, T.; Gleixner, A.; Heinz, S.; Vigerske, S. Analyzing the Computational Impact of MIQCP Solver Components. ZIB-Report 13-08 (February 2013). Available online: https://opus4.kobv.de/opus4-zib/frontdoor/index/index/searchtype/series/id/1/start/41/rows/100/facetNumber_year/all/yearfq/2013/docId/1775 (accessed on 19 September 2024).
39. Southern African Universities Radiometric Network (SAURAN). *Solar Radiometric Data for the Public*; Stellenbosch University Station (2018 Data): Stellenbosch, South Africa. Available online: https://sauran.ac.za/ (accessed on 27 February 2023).
40. Leyland, G.B. Multi-Objective Optimisation Applied to Industrial Energy Problems. Master's Thesis, University of Auckland, Auckland, New Zealand, 2002.
41. Gürler, H.E.; Özçalıcı, M.; Pamucar, D. Determining criteria weights with genetic algorithms for multi-criteria decision making methods: The case of logistics performance index rankings of European Union countries. *Socio-Econ. Plan. Sci.* **2024**, *91*, 101758. [CrossRef]
42. Abbaszadeh Shahri, A.; Shan, C.; Larsson, S.; Johansson, F. Normalizing Large Scale Sensor-Based MWD Data: An Automated Method toward A Unified Database. *Sensors* **2024**, *24*, 1209. [CrossRef] [PubMed]